Monthly Notices
of the
ROYAL ASTRONOMICAL SOCIETY

MNRAS **458,** 695–707 (2016)
Advance Access publication 2016 February 11

doi:10.1093/mnras/stw337

A core dynamo in Vesta?

M. Formisano,[1⋆] C. Federico,[1,2⋆] S. De Angelis,[1] M. C. De Sanctis[1⋆] and G. Magni[1]

[1]*INAF-IAPS, Via del Fosso del Cavaliere 100, I-00133 Roma, Italy*
[2]*Dipartimento di Fisica e Geologia, Universitá di Perugia, I-06123 Perugia, Italy*

Accepted 2016 February 9. Received 2016 February 9; in original form 2015 November 24

ABSTRACT

A recent study of Fu et al. analysed the remaining magnetization in the eucrite meteorite Allan Hills A81001, which mostly likely has been produced during the cooling phase of the life of the asteroid Vesta, arguing that an ancient dynamo in the advective liquid metallic core could be set in. Using petrographic and paleomagnetic arguments, Fu et al. estimated a surface magnetic field of at least 2 μT. In this work, we verify the possibility that an early core dynamo took place in Vesta by analysing four different possible fully differentiated configurations of Vesta, characterized by different chondritic compositions, with the constraints on core size and density provided by Ermakov et al. We only incorporate the thermal convection, by neglecting the effects of the compositional convection, so our results in terms of magnetic Reynolds number and duration of the dynamo can be interpreted as a lower bound. The presence of a magnetic field would make Vesta a peculiar object of the Solar system, a 'small-Earth', since it has also a differentiated structure like Earth and the magnetic field has preserved Vesta from the space weathering.

Key words: dynamo – planets and satellites: individual: Vesta – planets and satellites: interiors – planets and satellites: magnetic fields.

1 INTRODUCTION

The existence of planetary magnetic fields is strictly related to the occurrence and stability of a dynamo mechanism within the planetary core. Early solar nebula may have had a magnetic field, whose shape was dipolar with an intensity of about 100 μT (Levy & Sonett 1978), although this value has recently been updated and reduced to 5–54 μT (Fu et al. 2014b). The time-scale of free diffusive decay of a magnetic field within a planetary interior is given by $\tau_{\rm mag} = R^2/(\pi^2\lambda) \approx 3000\,{\rm yr}(R/10^3\,{\rm km})^2$ (Stevenson, Spohn & Schubert 1983; Stevenson 2010), where R is the planetary radius and λ is a constant: so $\tau_{\rm mag}$ is less than $\approx 10^3$–10^4 yr for an asteroid-sized body and is very short if compared with the age of Solar system (4.5×10^9 yr). Thus, the primordial magnetic fields of Solar system bodies are substantially absent at present time: the occurrence of a dynamo mechanism is required in order to sustain a magnetic field. The characteristic time-scale for thermal diffusion within a planet is given by $\tau_{\rm th} = R^2/(\pi^2\kappa) \approx (3 \times 10^8\,{\rm yr})(R/10^3\,{\rm km})^2$, with the thermal diffusivity $\kappa \approx 10(a_0 k_{\rm B} T/e^2)(\hbar/m)$ and the other parameters defined as a_0 (first Bohr radius), $k_{\rm B}$ (Boltzmann constant), T (temperature), e (electron charge), $\hbar$ (Planck constant divided by 2π); thus, τ_h is of the order of at least 10^8 yr for asteroids with size comparable to Vesta and Ceres, and it is even larger for most planets (Stevenson et al. 1983; Stevenson 2010). As a consequence, planetary interiors retain heat for very long times, and so high internal temperatures are maintained.

Typically, internal temperatures are reached that are well above the Curie point of most materials, so any permanent magnetization is lost everywhere except in the crust of the planet. Several conditions are required in order that a dynamo mechanism can be set in. First of all, a convection regime is required, which would imply a large magnetic Reynolds number and a small Rossby number. The planetary core must be characterized by electrical conductivity and fluidity. Nevertheless, the core must not be completely liquid, but it should be characterized by an inner solid core. The inner solid core must be embedded within a large fluid region, constituted by electrical conducting material in a non-uniform motion (Stevenson et al. 1983; Stevenson 2003, 2010). However, even in the absence of an inner solid core, a high heat flux at the core–mantle boundary could be assured by a more rapidly cooling core (Nimmo 2007). The electrical conductivity is guaranteed if both iron (or an iron alloy such as Fe-S) and a metallic material are present.

Magnetic fields have been measured on other Solar system objects in addition to Earth: among rocky bodies, Mercury is thought to have a weak dynamo, Venus, Moon and Mars likely have had an active dynamo in an ancient past, and Ganymede has an active current dynamo. Ice giants Jupiter, Saturn, Uranus and Neptune have active dynamos. Small bodies (i.e. asteroids) that experienced differentiation could have developed an active dynamo mechanism early in their history (Stevenson 2010), as we can see in Table 1.

⋆ E-mail: michelangelo.formisano@iaps.inaf.it (MF); costanzo.federico44@gmail.com (CF); mariacristina.desanctis@iaps.inaf.it (MCDS)

Table 1. Observed surface magnetic field of some bodies of the Solar system.

Body	Magnetic field (μT)	Reference
Vesta	>2.0	[A]
Earth (mean value)	50	[B]
Mars (mean value)[a]	50	[B]
Jupiter	428	[B]
Ganymede	2	[B]
Saturn	20	[B]
Uranus	20	[B]
Neptune	20	[B]

[a]The magnetic field of Mars is concentrated in well-defined regions. [A]: Fu et al. (2012); [B]: Stevenson (2010).

The theoretical time-scale for the duration of an active dynamo in the interior of planetesimals is of the order of 10–10^2 Myr after the Solar system formation (Elkins-Tanton, Weiss & Zuber 2011; Sterenborg & Crowley 2013). According to Elkins-Tanton et al. (2011) for example bodies with radii of the order of 100–150 km develop a dynamo lasting for a timespan ≥10 Myr, while bodies with radii of 300–350 km produce a dynamo lasting for a timespan ≥50 Myr.

Among the possible mechanisms to generate a dynamo, Monteux, Jellinek & Johnson (2011) suggest that a large impact on an initially undifferentiated body could release heat and induce the differentiation that leads to the generation of a transient dynamo inside the core. Nimmo (2009), moreover, suggests that compositional convection could play an important role in dynamo generation, providing a minimum core size of about 90 km.

The main observational evidence suggesting the existence of an ancient dynamo arises from measurements of remnant magnetization in meteorites (see for example Weiss et al. 2008a, 2010; Weiss, Lima & Zucolotto 2008b; Elkins-Tanton et al. 2011; Fu et al. 2012). The general idea is that few meteorites have retained records of primordial magnetic fields (related to the solar nebula or to the protoplanetary disc), and that the measured magnetizations are due to parent body internal field. For example, Fu et al. (2012) have investigated the natural remnant magnetization in a eucrite sample (ALHA81001). Petrographic and paleomagnetic arguments suggest that this eucrite sample acquired its residual magnetization about 3.69 Gyr ago, during its permanence in the Vestan crust: this magnetization is consistent with a surface magnetic field >2 μT, which was produced by a core magnetic field of the order of 10^2–10^3 μT. The presence of natural remnant magnetization on this eucrite is interpreted as due to a surface magnetic field generated by an ancient dynamo. Weiss et al. (2008b), analysing the three angrites Angra Dos Reis, D'Orbigny and Asuka (A)-881371, deduced that the remnant magnetization of the samples was possibly linked to an intrinsic dynamo, which generated an ancient magnetic field of the order of 10 μT on its parent body, about 4.5 Gyr ago, that decayed within 200–1600 Myr.

Core dynamo and, consequently, the magnetic field help to explain the lack of solar wind ion-generated space weathering effects on Vesta, as suggested by Fu et al. (2012). Irradiation experiments with Ar^{++} ions on Bereba eucrite (Vernazza et al. 2006), whose reflectance spectrum in the visible–near-infrared range is very similar to the one of Vesta, produced a darkening and reddening of the spectrum. This alteration is very similar to space weathering effects reproduced on silicates and meteorites in laboratory, and to what is observed on the Moon. In contrast, the spectra of Vesta do not show any lunar-like space weathering effect. Vernazza et al. (2006) conclude that a 0.2 μT surface magnetic field is responsible for the shielding from solar wind ions. The lack of any lunar-like observed space weathering effect on Vesta surface (Pieters et al. 2012) could also be a clue of the presence of a weak surface magnetic field.

A recent work (Toplis et al. 2013) has shown a wide range of possible Vesta-sized parent body, totally differentiated with a eucritic crust, based on mass balance and thermodynamic constraints. Following this paper, we have explored four different chondritic compositions, in order to evaluate how the composition and the size of the different layers (core, mantle and crust) affect the onset of a dynamo core inside Vesta and its magnetic core/surface field. The constraints on the size and density of the metallic core are provided by a recent paper (Ermakov et al. 2014) on the Vesta's gravity.

In this paper, we investigate the role of the thermal convection in the dynamo generation, neglecting the contribution of the compositional convection that can influence the energetic balance of the core and then the core flow velocities. As discussed by Nimmo (2009), a core dynamo can be activated also in the case of subadiabatic heat flow when compositional convection is included. For instance, by assuming typical Earth core parameters, the core compositional convective velocity is of a few mm s^{-1}: this velocity strongly depends on the density contrast and on the time of growing of the inner core (Nimmo 2009). In general, compositional convection is common among small body, as pointed out by Nimmo (2009) and Bryson et al. (2015), and the minimum likely core size for a dynamo driven by such convection is about 90 km (Nimmo 2009), very similar to the thermal convection analogous value found by Weiss et al. (2008a). Compositional convection is also associated with a long-lived magnetic activity in contrast with the thermal convection linked to a short-lived magnetization (Bryson et al. 2015). However, here we perform our calculations only in the thermal convection regime, and our results (magnetic Reynolds number and core dynamo duration) can be interpreted as a lower limit of the 'real' values.

We have organized this paper as follows: in Section 2 the physical parameters characterizing the inner structure of a fully differentiated Vesta are described, in Section 3 a parametrized convective model of a thermal evolving fully differentiated Vesta is described, in Section 4 the basic ideas and the equations of the dynamo theory applied to a small planetary object are reported, in particular deducing the equations for the intensity of the magnetic field and for the magnetic Reynolds number. In Sections 5 and 6, we describe and discuss the results looking for the onset of an ancient dynamo inside Vesta.

2 FULLY DIFFERENTIATED 'VESTAS'

We consider as a starting point a post-differentiated Vesta, i.e. an asteroid that has completed its differentiation due to the decay of the short-lived radionuclides and it is characterized by a metallic core, a silicate mantle and a crust.

If the requirement that the core heat flux is greater than zero is fulfilled, the onset of a dynamo in the core is possible. We can reasonably fix the temperatures of the core at 1200 K, of the mantle at 1600 K and of the crust at 500 K (Ghosh & McSween 1998). We have tested (see Section 5) that there are not significant differences in outcome if we use different initial temperatures, i.e. considering an hotter crust and a cooler mantle, as predicted by the work of Neumann, Breuer & Spohn (2014).

Among the different possible internal structures of a fully differentiated Vesta predicted by Toplis et al. (2013), we select four chondritic configurations in order to explore a wide range of core size (from 106 km in the case of CR composition to 143 km in

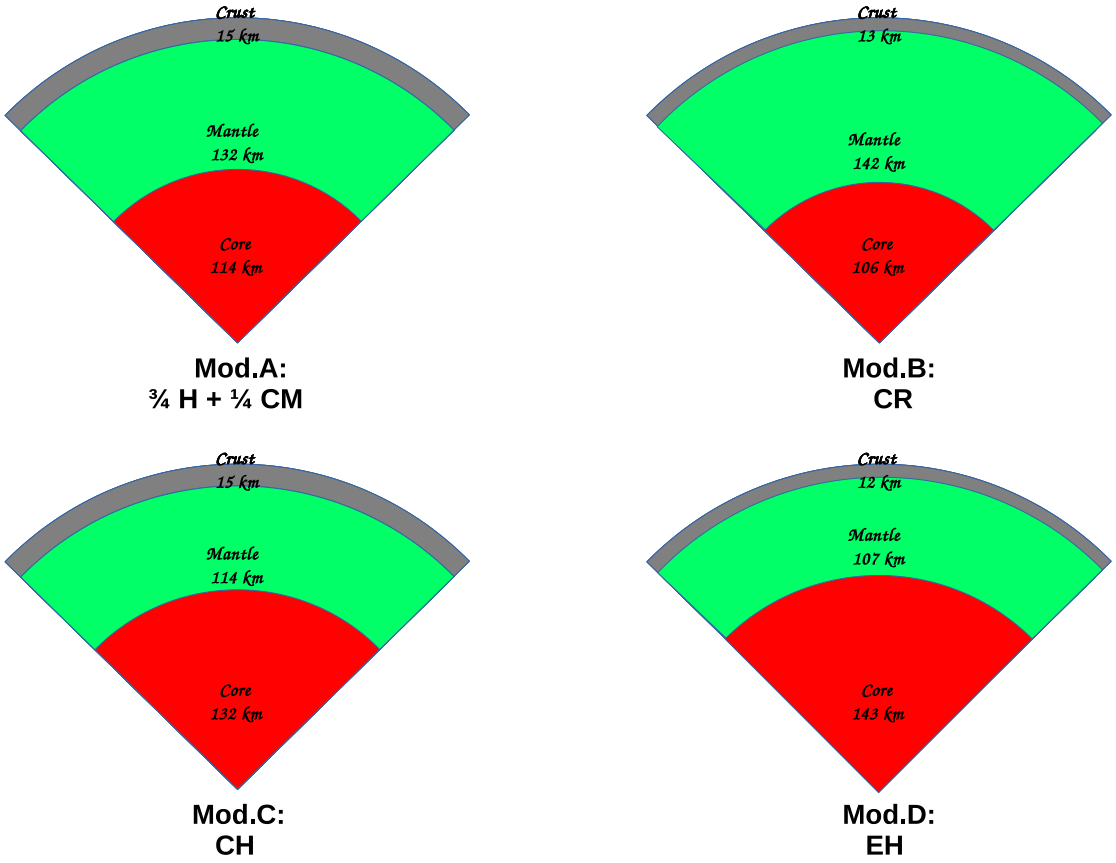

Figure 1. Internal structure for the four configurations selected in this paper: Mod. A refers to a plausible possible Vesta ($\frac{3}{4}$H + $\frac{1}{4}$CM chondrites; see Toplis et al. 2013). Mod. B, Mod. C and Mod. D refer to CR, CH and EH chondrites configurations, respectively.

Table 2. Thickness and density of the four different possible initial configurations of a fully differentiated Vesta (Toplis et al. 2013).

	Mod. A	Mod. B	Mod. C	Mod. D
	$\frac{3}{4}$H + $\frac{1}{4}$CM	CR	CH	EH
Thickness (km)				
Core	114.2	106.4	132.3	143.0
Mantle	132.4	142.2	113.8	107.0
Crust	15.0	13.0	15.4	11.6
Density (kg m^{-3})				
Core	6259	6175	7802	5786
Mantle	3266	3320	2861	3034
Crust	2885	2901	2533	2798

the case of EH composition). Toplis et al. (2013) consider the configuration characterized by $\frac{3}{4}$H + $\frac{1}{4}$CM chondrites as a plausible analogue of Vesta (see Toplis et al. 2013 for the details). Hereafter, this last model will be labelled Mod. A, while CR, CH and EH chondritic composition will be labelled Mod. B, Mod. C and Mod. D, respectively (see Fig. 1 and Table 2 for the details.) Note that CR and EH compositions are characterized by a core size slightly out of the range provided by Ermakov et al. (2014).

3 THE MODEL

In order to study the thermal evolution of Vesta, we applied the method of the parametrized thermal convection in which the different layers are characterized by a single temperature and conservation of energy is imposed. The method of parametrized convection is largely diffused in the literature in order to study the thermal evolution of planets/planetesimals (Schubert 1979; Stevenson et al. 1983; McNamara & van Keken 2000; Solomatov & Moresi 2000; Korenaga & Jordan 2002; Freeman 2006; Grindrod et al. 2007; Korenaga 2009; Sterenborg & Crowley 2013). Following this approach, we solve this system of first-order differential equations:

$$\begin{cases} \left(V\rho c_{\rm p}\right)_{\rm c} \dfrac{{\rm d}T_{\rm c}}{{\rm d}t} = -F_{\rm out}A_{\rm top,c} \\ \left(V\rho c_{\rm p}\right)_{\rm m} \dfrac{{\rm d}T_{\rm m}}{{\rm d}t} = F_{\rm in}A_{\rm bottom,c} - F_{\rm out}A_{\rm top,m} + Q(t)V_{\rm m} \\ \left(V\rho c_{\rm p}\right)_{\rm cr} \dfrac{{\rm d}T_{\rm cr}}{{\rm d}t} = F_{\rm in}A_{\rm bottom,m} - F_{\rm out}A_{\rm top,cr}, \end{cases} \quad (1)$$

where $T_{\rm c}$, $T_{\rm m}$ and $T_{\rm cr}$ are, respectively, the temperature of the core, of the mantle and of the crust, V is the volume of the layer, ρ is the density, $c_{\rm p}$ is the specific heat, F is the heat flux, A is the area of the layer and Q is the radiogenic heat production per unit volume.

The radiogenic heat provided by long-lived radionuclides, i.e. ^{235}U, ^{238}U, ^{232}Th and ^{40}K and given by Turcotte & Schubert (2002), and reported in Table 3, is

$$Q(t) = \sum_{i=1}^{n} Q_i C_{0,i} \exp\left(-\lambda_i t\right), \quad (2)$$

Table 3. Radiogenic heating parameters used in this model are provided by Turcotte & Schubert (2002).

Element	Initial concentration (C_i) (ppb)	Specific heat production (Q_i) (W kg^{-1})	Half-lives (λ_i) [Ga]
^{238}U	62.4	9.46×10^{-5}	4.47
^{235}U	16.4	56.90×10^{-5}	0.70
^{232}Th	155.0	2.64×10^{-5}	14.0
^{40}K	463.6	2.92×10^{-5}	1.25

where Q_i is the heat production of the species i, $C_{0,i}$ is the initial abundance and λ_i is the decay constant [values provided by Turcotte & Schubert (2002)]. The heat flux in equation (1) is given by

$$F = \frac{K\Delta T}{D}\mathrm{Nu}, \tag{3}$$

where K is the thermal conductivity, ΔT is the temperature drop over the boundary layer, D is the thickness of the layer and Nu is the Nusselt number. In the parametrized convection, the Nusselt number quantifies how much the convection is 'strong' with respect to the conduction, and it is linked to the thermal boundary layer (δ) by the following equation (Solomatov & Moresi 2000):

$$\delta = D/\mathrm{Nu}. \tag{4}$$

The Nusselt number can also be linked to Rayleigh number (Ra) through a relationship, by approximating the results obtained in different convection regimes, using numerical simulations:

$$\mathrm{Nu} = a\theta^b \mathrm{Ra}^c. \tag{5}$$

In fact, a, b and c depend on the convection regime we select. In a regime of variable viscosity Newtonian stagnant-lid scaling law (Moresi & Solomatov 1995), Nusselt number is related to Rayleigh number by the following relationship:

$$\mathrm{Nu} = 1.89\theta^{-1.02}\mathrm{Ra}^{0.2}. \tag{6}$$

We can write the Rayleigh number as (Solomatov 1995)

$$\mathrm{Ra} = \frac{\alpha g \rho \Delta T D^3}{\kappa \eta}, \tag{7}$$

where α is the thermal expansion, g is the gravity acceleration and κ is the thermal diffusivity. In the stagnant-lid regime (Solomatov & Moresi 2000), the Frank-Kamenetskii θ parameter is given by

$$\theta = \ln(\Delta\eta), \tag{8}$$

where $\Delta\eta$ is the viscosity contrast. We use a viscosity law not only dependent on the average temperature (T) of the layer (see, for example, Grindrod et al. 2007), but also on melting degree (Sterenborg & Crowley 2013):

$$\eta = \eta_0 \exp\left[\frac{E}{RT_{\mathrm{melt}}}\left(\frac{T_{\mathrm{melt}}}{T} - 1\right)\right]\exp[-C\chi], \tag{9}$$

where η_0 is the viscosity of the material at the zero pressure melting point (i.e. the reference viscosity), T_{melt} is the melting temperature of the layer, E is the activation energy, R is the gas constant, C is the melt constant [for the mantle we set this value at 25, which corresponds to the case of diffusion creep (Reese & Solomatov 2006)] and χ is the melting degree defined as (Reese & Solomatov 2006)

$$\chi = \frac{T - T_{\mathrm{sol}}}{T_{\mathrm{liq}} - T_{\mathrm{sol}}}, \tag{10}$$

where T_{sol} and T_{liq} are the solidus and liquidus temperature of the layer, respectively. We can rewrite equation (8) as

$$\theta = \frac{E\Delta T}{RT^2}. \tag{11}$$

The melting temperatures (T_{melt}) for silicate and metallic component are those corresponding at the 50 per cent of the melting (see Table 4), by assuming that temperature linearly depends on the melting degree. In a first modelling, we assume isoviscosity (0.01 Pa s) in the core. Successively, we explore the case in which core has a viscosity temperature dependence. Crust is assumed conductive.

All physical parameters used in our modelling are reported in Table 4.

3.1 Boundary conditions

For each layer (n), the heat flow across the boundaries is calculated as follows (McNamara & van Keken 2000; Freeman 2006):

$$F_{n,\mathrm{in}} = F_{n-1,\mathrm{out}}. \tag{12}$$

The flux entering in the core is set to zero. At surface, a fixed temperature (270 K) is used.

4 DYNAMO THEORY BASICS

4.1 'Dynamo effect'

Before introducing the magnetic Reynolds number, we want to recall some basic ideas and equations about the theory of a planetary dynamo. The presence of a dynamo inside an asteroid is linked to a moving conductive liquid core that generally is made of metallic material. The metallic core is the result of the physical differentiation that occurs in the first stages of the life of these bodies. In Formisano et al. (2013), we analysed the differentiation of Vesta, induced by the heat released by the radiogenic sources (in particular ^{26}Al).

Suppose that a poloidal magnetic field exists and some of the lines of this field are 'trapped' in the rotating fluid core. Since the rotation of the core is not uniform, these lines are deformed in the direction perpendicular to the rotation axis and they create a toroidal magnetic field. As the core rotates, these lines wrap themselves increasingly as far as to create a very intense field. Convective cells carry the lines of the magnetic field, and the Coriolis force deflects the fluid that starts to spin around the central axis of the cell. At this point, small loops are generated and subsequently they merge in a single large loop and re-create a strong poloidal magnetic field.

4.2 The magnetic induction equation

Here we deduce the magnetic induction equation, from which it is possible to define the magnetic Reynolds number that controls 'the efficiency' of a dynamo. In order to explain the dynamo theory,

Table 4. References. [A]: Russell et al. (2012); [B]: JPL Small-Body Database; [C]: Monteux et al. (2011); [D]: Sterenborg & Crowley (2013); [E]: Yoshino, Walter & Katsura (2004); [F]: Neumann et al. (2014); [G]: Ellsworth & Schubert (1983); [H]: Fraeman & Korenaga (2010).

Parameter		Value	Units	Ref.
Mass	M	2.6×10^{20}	(kg)	[A]
Rotational period	P	5.34	(h)	[B]
Surface temperature	$T_{\rm surf}$	270	(K)	–
Surface gravity	$g_{\rm surf}$	0.25	($\rm m\ s^{-2}$)	–
Gravitational constant	G	6.67×10^{-11}	($\rm m^3\ kg^{-1}\ s^{-2}$)	–
Gas constant	R	8.3144	($\rm J\ mol^{-1}\ K^{-1}$)	–
Stefan–Boltzmann constant	σ	5.67×10^{-8}	($\rm W\ m^{-2}\ K^4$)	–
Vacuum permeability	μ_0	$4\pi \times 10^{-7}$	($\rm N\ A^{-2}$)	[D]
Specific heat capacity of core	$c_{\rm p,c}$	800	($\rm J\ kg^{-1}\ K^{-1}$)	[C]
Thermal conductivity of core	$K_{\rm c}$	40.0	($\rm W\ m^{-1}\ K^{-1}$)	[C]
Thermal expansivity of core	$\alpha_{\rm c}$	1.5×10^{-5}	($\rm K^{-1}$)	[C]
Solidus temperature of core	$T_{\rm c,sol}$	1213	(K)	[F]
Melting of 50 per cent of core[a]	$T_{\rm c,50}$	1450	(K)	–
Liquidus temperature of core	$T_{\rm c,liq}$	1700	(K)	[F]
Reference viscosity of core	$\eta_{\rm 0,c}$	10^{14}	(Pa s)	[G]
Magnetic diffusivity of core	$\lambda_{\rm c}$	2	($\rm m^{-2}\ s^{-1}$)	[C]
Specific heat capacity of mantle	$c_{\rm p,m}$	1250	($\rm J\ kg^{-1}\ K^{-1}$)	[G]
Thermal conductivity of mantle	$K_{\rm m}$	4.2	($\rm W\ m^{-1}\ K^{-1}$)	[G]
Thermal expansivity of mantle	$\alpha_{\rm m}$	4×10^{-5}	($\rm K^{-1}$)	[D]
Reference viscosity of mantle	$\eta_{\rm 0,m}$	10^{19}	(Pa s)	[H]
Solidus temperature of mantle	$T_{\rm m,sol}$	1425	(K)	[F]
Melting of 50 per cent of mantle[a]	$T_{\rm m,50}$	1638	(K)	–
Liquidus temperature of mantle	$T_{\rm m,liq}$	1850	(K)	[F]
Activation energy of mantle	E	300	($\rm kJ\ mol^{-1}$)	[H]

[a]This value is calculated assuming that temperature linearly depends on degree of melting. Except for the thickness and for the density, crust physical parameters are the same as used for the mantle.

some of the basic equations of the classical electromagnetism are required. The starting equations are Ohm's law:

$$\boldsymbol{J} = \sigma\,[\boldsymbol{E} + \boldsymbol{u} \times \boldsymbol{B}]\,, \tag{13}$$

Ampere's law:

$$\nabla \times \boldsymbol{B} = \mu_0 \boldsymbol{J}, \tag{14}$$

and Faraday's law:

$$\nabla \times \boldsymbol{E} = -\frac{\partial \boldsymbol{B}}{\partial t}, \tag{15}$$

where $\boldsymbol{J}$ is the current density, σ the electrical conductivity, $\boldsymbol{E}$ the electric field, $\boldsymbol{B}$ the magnetic induction, $\boldsymbol{u}$ the velocity of the conducting fluid with respect to the planet and μ_0 is the magnetic permeability of free space. The parameters σ and μ_0 are related by:

$$\lambda = \frac{1}{\mu_0 \sigma}, \tag{16}$$

where λ is the magnetic diffusivity. The magnetic diffusivity is generally set to $2\ \rm m^2\ s^{-1}$ in the terrestrial planet in order to take into account the presence of other elements (e.g. sulphur) in the liquid metallic iron core (Stevenson 2003). Taking the curl of Ohm's law (see equation 13), in the assumptions of constant conductivity (σ), we obtain

$$\nabla \times \boldsymbol{J} = \sigma \nabla \times \boldsymbol{E} + \sigma \nabla \times (\boldsymbol{u} \times \boldsymbol{B})\,. \tag{17}$$

Taking the curl of Ampere's law (equation 14):

$$\nabla \times \boldsymbol{J} = \frac{1}{\mu_0} \nabla \times (\nabla \times \boldsymbol{B})\,, \tag{18}$$

we can rewrite equation (17) as follows:

$$\nabla \times (\nabla \times \boldsymbol{B}) = \mu_0 \sigma \nabla \times \boldsymbol{E} + \mu_0 \sigma \nabla \times (\boldsymbol{u} \times \boldsymbol{B})\,. \tag{19}$$

Using Faraday's law (equation 15), we obtain

$$\nabla \times (\nabla \times \boldsymbol{B}) = -\mu_0 \sigma \frac{\partial \boldsymbol{B}}{\partial t} + \mu_0 \sigma \nabla \times (\boldsymbol{u} \times \boldsymbol{B})\,. \tag{20}$$

Now, we rewrite the left term by applying the standard vector identity:

$$\nabla \times (\nabla \times \boldsymbol{B}) = \nabla\,(\nabla \cdot \boldsymbol{B}) - \nabla^2 \boldsymbol{B} = -\nabla^2 \boldsymbol{B}, \tag{21}$$

where we used Gauss's law for magnetism, and we obtain

$$\frac{\partial \boldsymbol{B}}{\partial t} = \nabla \times (\boldsymbol{u} \times \boldsymbol{B}) + \lambda \nabla^2 \boldsymbol{B}. \tag{22}$$

Notice that we have used the definition of the magnetic diffusivity (equation 16). Equation (22) is called *magnetic induction equation*. The first right term of equation (22) is the driving force and the second right term is the dissipative force: if the driving term is much larger than the dissipative one, the generation of a dynamo is possible. Otherwise the field 'diffuses' away and decays on a time-scale of (Stevenson 2003)

$$\tau \sim \frac{L^2}{\pi^2 \lambda} \sim (3000\ \rm yr) \left(\frac{R_{\rm c}}{1000\ \rm km}\right)^2 \left(\frac{1\ \rm m^2}{s\lambda}\right). \tag{23}$$

In the case of Vesta, this time-scale is very short and ranges from 18 to 29 yr [using the lowest (110 km) and highest (138 km) possible values for the core size (Ermakov et al. 2014)].

4.3 Onset of core dynamo

The magnetic Reynolds number is the ratio of the first to the second term on the right-hand side of equation (22):

$$\rm Re_m = \frac{\nabla \times (\boldsymbol{u} \times \boldsymbol{B})}{\lambda \nabla^2 \boldsymbol{B}} \approx \frac{u_{\rm c} B / R_{\rm c}}{\lambda B / R_{\rm c}^2} \approx \frac{u_{\rm c} R_{\rm c}}{\lambda}, \tag{24}$$

where u_c is the core convection velocity and R_c is the core radius. As pointed out by Christensen (2010), three different scaling laws exist for the velocity u_c, based upon

(i) the mixing-length theory (hereafter MIX);
(ii) the MAC-balance estimate (magnetic, Archimedean and Coriolis forces);
(iii) the CIA-balance estimate (Coriolis, inertia and Archimedean forces).

Since velocities in the MIX and CIA theory are of the same orders of magnitude (Weiss et al. 2010), we choose to analyse the MIX and MAC cases. As already discussed in Monteux et al. (2011), since the rotation rate of a primordial asteroid is a not well-constrained parameter, a value for the velocity can reasonably be chosen applying the balance between the inertial and buoyancy force. Following Stevenson (2003) and Christensen & Aubert (2006), the core convection velocity ($u_{c,\,MIX}$) is defined, in the mixing-length theory, by the relationship

$$u_{c,MIX} = \left(\frac{R_c F_{conv}}{\rho H_T}\right)^{1/3}, \tag{25}$$

with $H_T = c_{p,\,c}/\alpha_c g_c$, and α_c is the thermal expansivity of the core, F_{conv} is the core convective flux, $c_{p,c}$ is the specific heat, ρ_c is the density of the core and the core gravity acceleration is given by

$$g_c = \frac{4\pi G \rho_c R_c}{3}, \tag{26}$$

where G is the gravitational constant. Finally, we can rewrite equation (25) as (Christensen 2010)

$$u_{c,MIX} = \left(\frac{4\pi G \alpha_c R_c^2 F_{conv}}{3 c_{p,c}}\right)^{1/3}. \tag{27}$$

We have assumed that the mixing length corresponds to the core size (Stevenson 2010). In the case of MAC theory, the convective velocity of core is given by (Christensen & Aubert 2006)

$$u_{c,MAC} = \left(\frac{F_{conv}}{\rho_c \omega H_T}\right)^{1/2}, \tag{28}$$

where ω is the angular velocity [we assume the value 3×10^{-4} s^{-1} (Weiss et al. 2010), even if this value is not necessarily the 'primordial' value]. Fu et al. (2014a) estimated that Vesta had a rotation period 6.3 per cent faster than present before two late giant impact. However, we can reasonably assume that the past rotation rate is very similar to today.

We can arrange equation (28) as (Weiss et al. 2010; Sterenborg & Crowley 2013)

$$u_{c,MAC} = \left(\frac{4\pi G \alpha_c R_c F_{conv}}{3\omega c_{p,c}}\right)^{1/2}. \tag{29}$$

See Table 4 for the physical parameters used in this work. Now, we can derive another expression for the magnetic Reynolds number, in both MIX and MAC cases. In the MIX case, using equation (27), we can write

$$Re_{m,MIX} = \left(\frac{4\pi G \alpha_c F_{conv} R_c^5}{\lambda^3 c_{p,c}}\right)^{1/3}, \tag{30}$$

while in MAC case, using equation (29), we obtain

$$Re_{m,MAC} = \left(\frac{4\pi G \alpha_c F_{conv} R_c^3}{3\omega c_{p,c} \lambda^2}\right)^{1/2}. \tag{31}$$

The convective core heat flux is calculated as

$$F_{conv} = F_c - F_{cond}, \tag{32}$$

using Sterenborg & Crowley (2013), where F_c is given by

$$F_c = K_c \frac{(T_c - T_m)}{\delta_b}, \tag{33}$$

where K_c is the core thermal conductivity, and δ_b is the thermal boundary layer between the core and the mantle. In Sterenborg & Crowley (2013), it is assumed that δ_b is equal to δ_u, which is a thin layer between the mantle and the crust where the drop of viscosity occurs, and the core heat flux does not depend on core viscosity. Successively, we explore the case in which the core has a temperature-dependent viscosity. Following the approach of Sterenborg & Crowley (2013), the condition for the onset of convection inside the core of Vesta is set by the requirement that the heat flux coming out of the core exceeds the heat flux along the adiabatic, i.e. the conductive heat flux, defined by (Stevenson 2003)

$$F_{cond} = \frac{K_c \alpha_c g_c T_c}{c_{p,c}}. \tag{34}$$

So, if $F_c > F_{cond}$ (i.e. $F_{conv} > 0$), the core begins to convect, but it is not sufficient to maintain a magnetic field, since the induction effect must 'win' against the diffusive losses: this indication is given by the magnetic Reynolds number, which must exceed a critical value. Using equation (33), we can rewrite equations (30) and (31) as

$$Re_{m,MIX} = \left(\frac{4\pi K_c G \alpha_c R_c^5 (T_c - T_m)}{\lambda^3 c_{p,c} \delta_b}\right)^{1/3}, \tag{35}$$

and

$$Re_{m,MAC} = \left(\frac{4\pi K_c G \alpha_c R_c^3 (T_c - T_m)}{3\omega c_{p,c} \lambda^2 \delta_b}\right)^{1/2}. \tag{36}$$

In some papers (Olson & Christensen 2006), the critical value is set to $Re_{m,\,CRI} = 40$, while in others (Christensen, Olson & Glatzmaier 1999; Christensen & Aubert 2006; Monteux, Jellinek & Johnson 2011) it is inside the range 10–100. In this work, we set the critical value at 50. The magnetic energy field strength of a dynamo is provided by (Christensen 2010)

$$\frac{B_c^2}{2\mu_0} = f_{ohm} \frac{\tau F_{conv} \alpha_c g_c}{c_{p,c}}, \tag{37}$$

where f_{ohm} is the fraction of the available power that is converted to magnetic energy and τ is the ohmic dissipation time. Following Sterenborg & Crowley (2013), we set $f_{ohm} = 1$. Since $\tau = R_c/u_c$, we can rewrite equation (37) and provide a formula for the magnetic field on the core:

$$B_c^2 = \left(\frac{2\mu_0 R_c \alpha_c g_c F_{conv}}{u_c c_{p,c}}\right)^{1/2}. \tag{38}$$

Using equation (26), we can rewrite equation (38) as

$$B_c^2 = \left(\frac{2\mu_0 \rho_c}{u_c}\right)\left(\frac{4\pi G \rho_c R_c^2 F_{conv}}{3 c_{p,c}}\right). \tag{39}$$

In the case of MIX theory, using equation (27), we can obtain (Sterenborg & Crowley 2013)

$$B_{c,MIX} = \sqrt{2\mu_0 \rho_c u_{c,MIX}^2}. \tag{40}$$

This is the magnetic core field intensity in the case of mixing-length theory. If we use the MAC scaling law (equation 29), we obtain (Weiss et al. 2010; Sterenborg & Crowley 2013)

$$B_{c,MAC} = \sqrt{2\mu_0 R_c \rho_c \omega u_{c,MAC}}. \tag{41}$$

In the dipole field approximation, we can calculate the magnetic field at the surface. Following Christensen & Aubert (2006), we obtain

$$B_{\rm surf} = 0.8 B_{\rm c} \left(\frac{R_{\rm c}}{R} \right)^3, \tag{42}$$

which gives an estimation of the surface magnetic field in the assumption that the dipole field at the core–mantle boundary is about 80 per cent of the total magnetic field. We also compute the Rossby number, defined as

$$\mathrm{Ros} = \frac{u_{\rm c}}{\omega R_{\rm c}}. \tag{43}$$

The Rossby number is the ratio between inertial and Coriolis forces: when Coriolis dominates, the field tends to be dipolar, otherwise it tends to be multipolar (Weiss et al. 2010). In particular, if Rossby number is >0.12, the field is multipolar, otherwise it is dipolar (Weiss et al. 2010).

5 RESULTS

In this section, we will discuss the results of our modelling, in particular the magnetic Reynolds number and the magnetic field intensity (both for core and surface) time evolution. Our reference model setup will be Mod. A, with core convective velocity provided by the mixing-length theory. Here, we explore how a different scaling law (MAC) for core convective velocity and different initial chondritic configurations (Mod. B, Mod. C and Mod. D) could affect the results in terms of magnetic Reynolds number and magnetic field. Finally, we discuss how a change in the core viscosity can affect the intensity of the magnetic field.

5.1 Mod. A

In Mod. A, which corresponds to a likelihood configuration of Vesta (Toplis et al. 2013), the core temperature first reaches and then overcomes the mantle one after about 30 Myr (Fig. 2a). Successively, both temperatures reach the same asymptotic value after 300 Myr. Mantle temperature is affected by the cooling action of the convection while the contribution of the long-lived radionuclides is not sufficient to raise the temperature in the layer, since their efficiency is low in the considered time-scale. Core temperature initially increases to reach the thermodynamic equilibrium with the hotter mantle. The mantle viscosity follows the exponential law of equation (9), starting from an initial value of 10^{14} Pa s, which corresponds to a partial melted mantle till to a higher value, 10^{19} Pa s, typical of the silicate solid rocks (Fraeman & Korenaga 2010, see Fig. 2b). This high value remains constant for all the timespan of the simulation. Recall that we assume isoviscosity in the core and in the crust. In Fig. 2(c), we report the fluxes coming out from the different layers and the core adiabatic heat flux, which generally lies in the range from 0.13 to 7.3 mW m^{-2}, using typical parameter values for small body (Weiss et al. 2010). When heat flux from the core overcomes the adiabatic heat flux (after about 30 Myr), the convection in the core starts.

The maximum heat core flux value reached is 10 mW m^{-2}, while the fluxes of the mantle and of the crust decrease from an initial higher value (100 mW m^{-2}) to an almost constant value of 20 mW m^{-2}. In Fig. 2(d), we report the Nusselt number in the mantle which is higher than 1 when convection is acting: convection in the mantle stops after about 10 Myr. The requirement of a heat core flux higher than the adiabatic value is not sufficient to make possible the dynamo: it is also required that the magnetic field do not diffuse away and it implies that the magnetic Reynolds number must overcome a critical value that we have arbitrarily chosen to be equal to 50 (Fig. 2e). In fact, the grey box in the plot indicates the region of all possible predicted critical magnetic Reynolds numbers, which range from 10 to 100. If the magnetic Reynolds number is lower than the critical value, the dissipative forces inhibit the dynamo. So the dynamo is active until the magnetic Reynolds number is greater than that value. The intersection between green line (the magnetic Reynolds numbers coming out from our modelling) and red line (critical value) can be interpreted as the end point of the dynamo. From Fig. 2(e), the duration is about 150 Myr. In Fig. 2(f), the intensity of magnetic field of the core and surface is reported. The maximum intensity reached when dynamo was active is about 100 μT for the core and few μT for the crust, according to equation (42). Remember that if the magnetic Reynolds number is higher than 1, we have a perfectly conducting plasma, and the lines of the magnetic field are frozen in the plasma (*Alfvén's frozen in theorem*).

5.1.1 *Dependence on velocity scaling law*

Different scaling laws for convective velocity in the core lead to different results in magnetic Reynolds number and intensity of the magnetic field. As stated by Weiss et al. (2010), in general, $u_{\rm c,MIX}$ is greater than $u_{\rm c,\,MAC}$ of one to two orders of magnitude, and this implies high magnetic Reynolds number in the case of mixing-length theory, as we can see in Figs 2(e) and 3(a) (Weiss et al. 2010). In Figs 4(a) and (b), we have considered an intermediate case between MIX and MAC approaches, by simply arithmetically averaging the convective core velocities in the two cases.

In the MAC case, the magnetic fields are about one order of magnitude greater than MIX one (Figs 2 f and 3b) and the magnetic Reynolds number is around 0 (Fig. 3a): in this case, the magnetic field will diffuse away. The intermediate case is characterized by a magnetic Reynolds number always inside the 'box' of the critical values, but below 50 (Fig. 4a), while the intensity of the magnetic fields is very similar to the MIX case (Figs 2f and 4b). Anyway, we have to discard the results of the MAC scaling law since the requirement for the existence of MAC balance (Starchenko & Jones 2002):

$$\frac{u_{\rm c} R_{\rm c}}{\lambda} > 50 \tag{44}$$

is not met. In fact, substituting the calculated core velocity and size, we obtain values around 1. So, in the case of Vesta, the magnetostrophic balance between Coriolis, pressure, buoyancy and Lorentz forces is not assured, and in this case the MAC regime is not valid.

In Fig. 5(a), the time evolution of the convective core velocity in the three cases we considered is reported and, effectively, core velocity in the mixing-length theory is the highest. The Rossby number is always very small and lower than 0.12, and this indicates that the nature of the magnetic field is dipolar (Fig. 5b).

5.1.2 *Dependence on the initial temperature values*

If we vary the initial temperature of the crust and mantle, the values and the trend of the Reynolds magnetic number and of the intensity of the magnetic field do not change. We have used as test case Mod. A: we choose for the mantle and the crust initial temperatures of 1400 and 700 K, respectively. In this case, the maximum magnetic Reynolds number is 56.1. If we choose 1500 and 600 K as the initial

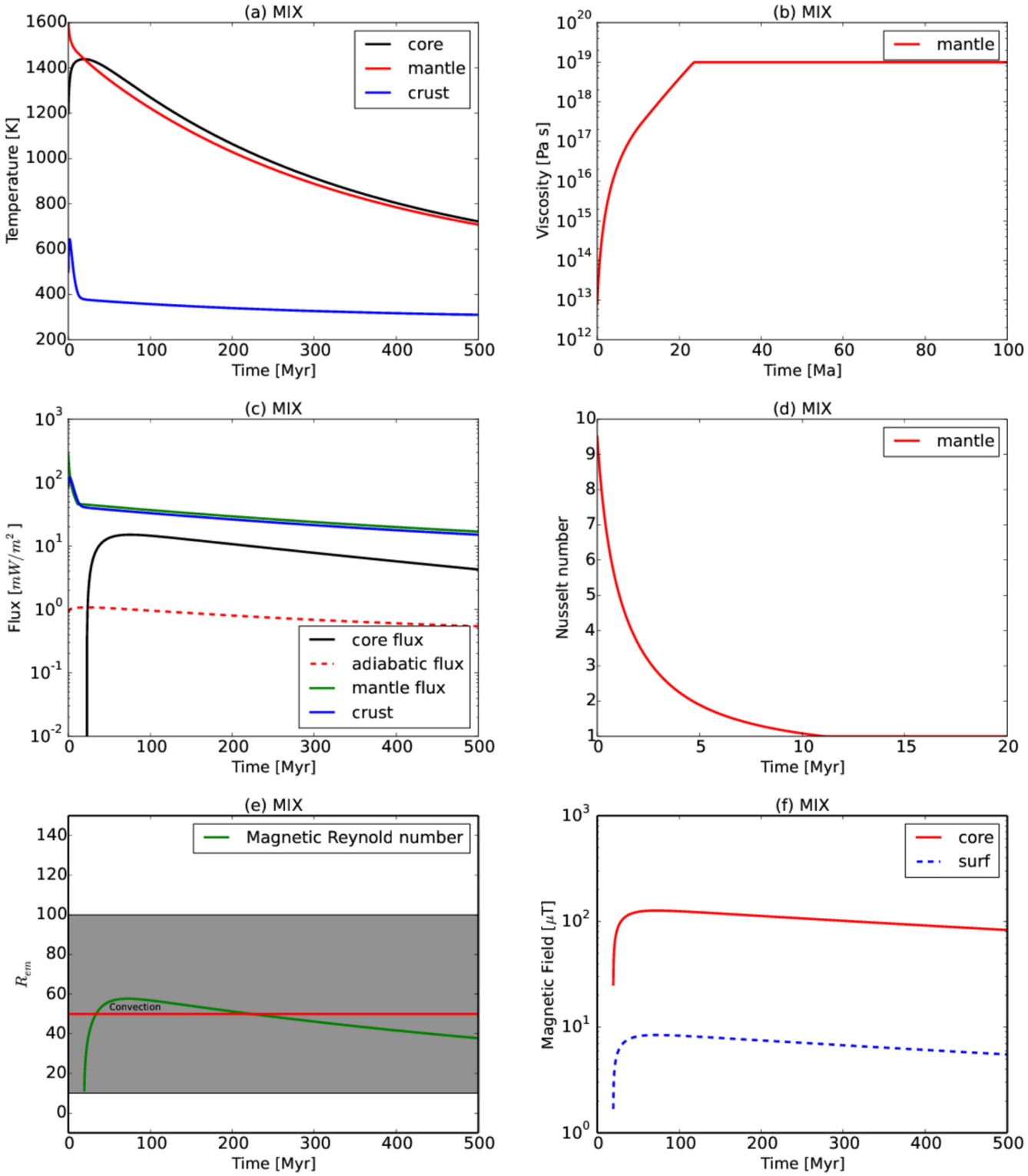

Figure 2. Time evolution of (a) temperature of different layers, (b) viscosity of mantle, (c) flux coming out of different layers and adiabatic core flux, (d) Nusselt number of mantle, (e) magnetic Reynolds number, (f) magnetic field intensity, in the case of Mod. A and mixing-length theory scaling law for core convective velocity. Grey box ranges from 10 to 100 which are the typical minimum and maximum values of the critical number we found in the literature. In our work, we set the critical value at 50 (red line). Since viscosity becomes constant after 30 Myr, we reduce the *x*-axis up to 100 Myr (b). For an analogous reason, we reduce the *x*-axis up to 20 Myr for the Nusselt number time evolution (d).

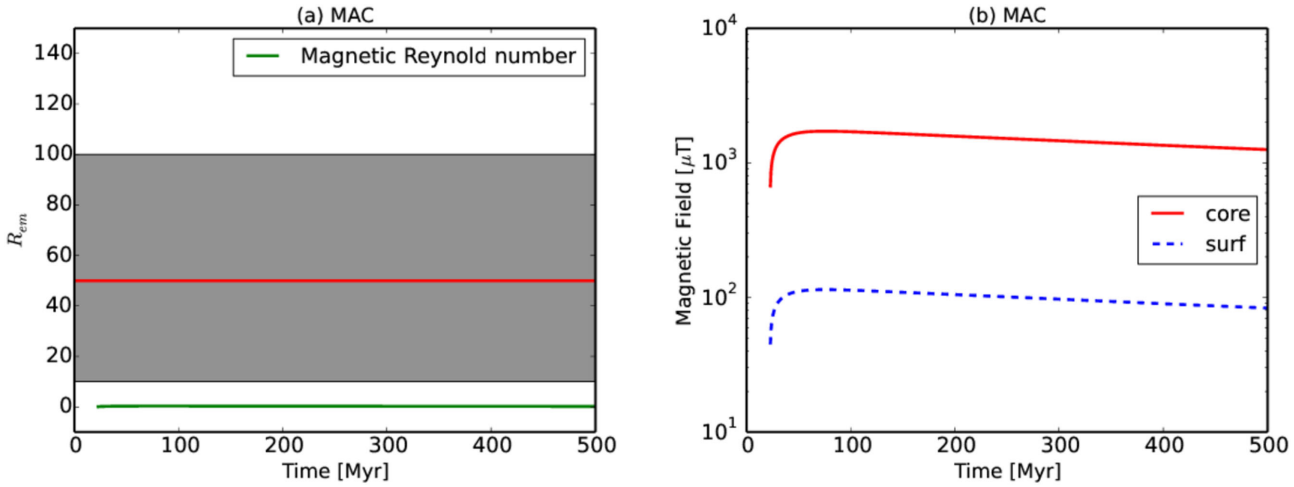

Figure 3. (a) Magnetic Reynolds number and (b) magnetic field intensity evolution in time, in the case of MAC scaling law. Grey box ranges from 10 to 100 which are the typical minimum and maximum values of the critical number we found in the literature. In our work, we set the critical value at 50 (red line).

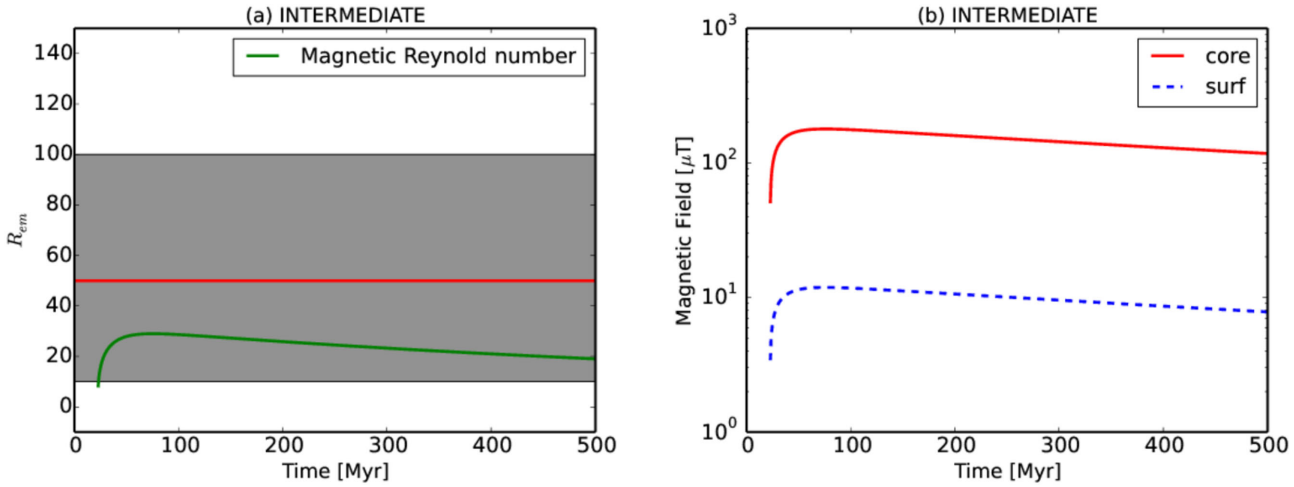

Figure 4. (a) Magnetic Reynolds number and (b) magnetic field intensity evolution in time, in an intermediate case between mixing-length theory and MAC scaling law. Grey box ranges from 10 to 100 which are the typical minimum and maximum values of the critical number we found in the literature. In our work, we set the critical value at 50 (red line).

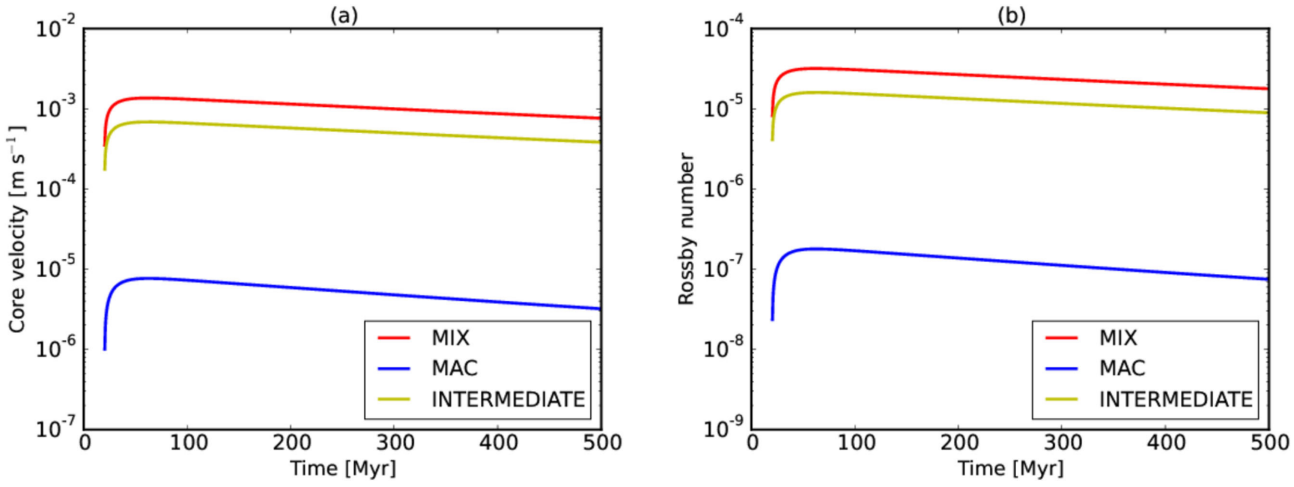

Figure 5. (a) Core velocity time evolution and (b) Rossby number time evolution for the different scaling laws we explored.

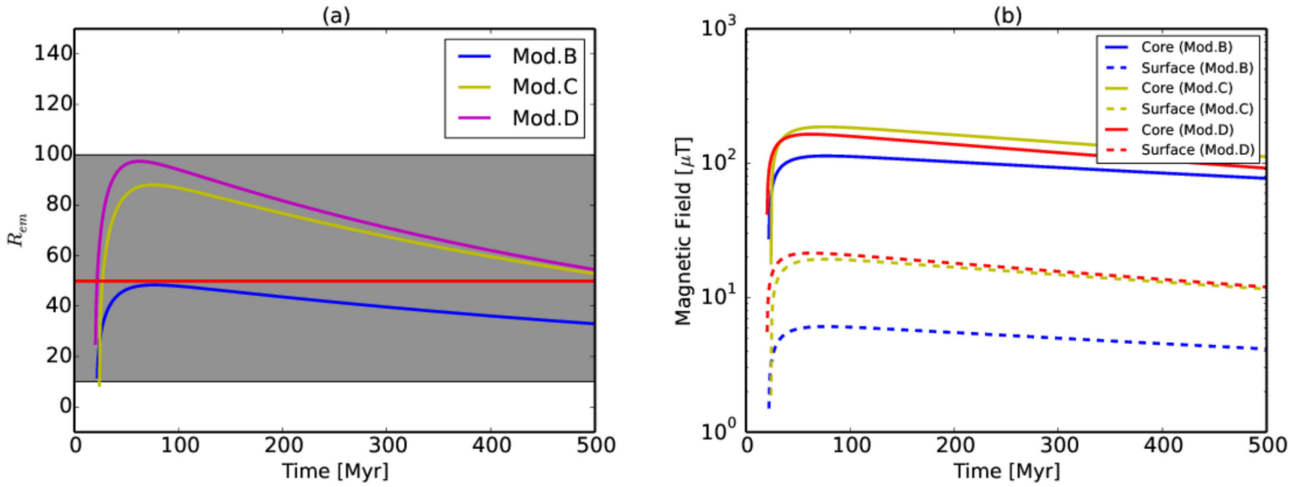

Figure 6. (a) Magnetic Reynolds number and (b) magnetic field intensity for Mod. B, Mod. C and Mod. D. Grey box ranges from 10 to 100 which are the typical minimum and maximum values of the critical number we found in the literature. In our work, we set the critical value at 50 (red line).

temperatures of the mantle and crust, respectively, the maximum magnetic Reynolds number is 54. These results indicate that the dynamo duration is not significantly affected by the choice of the initial temperatures. Also the intensity of the magnetic field does not change.

5.2 Dependence on the internal structure (Mod. B, C and D)

We have tested the change in the magnetic Reynolds number and in the magnetic field due to different internal structures. These configurations are constrained by chemical and petrological (Toplis et al. 2013) as well as gravity considerations (Ermakov et al. 2014). The model with the smaller core, i.e. Mod. B, is characterized by a magnetic Reynolds number always lower than the critical value that means that the dynamo does not occur (Fig. 6a). The corresponding maximum core magnetic field intensity is slightly lower than 100 μT (Fig. 6b). In the other two cases, Mod. C and Mod. D, the magnetic Reynolds number overcomes the critical value up to about 500 Myr, which corresponds (more or less) also at the dynamo duration (Fig. 6a). In both cases, the core magnetic field overcomes 10^2 μT, while the surface magnetic field is around 2–3 μT (Fig. 6b).

5.3 Temperature-dependent core viscosity (Mod. A)

In this section, we show how the results in terms of magnetic field and magnetic Reynolds number change if we consider a temperature-dependent core viscosity: for simplicity, we consider only Mod. A in the mixing-length case. The temperature profile for the core and the mantle is essentially the same: in fact, they reach the thermal equilibrium after 20 Myr (Fig. 7a). The peculiarity of this model is that the viscosity reaches very low values (10^{-2}–10^{-3} Pa s), the typical values used in the literature for the 'liquidus' (see, e.g., Yoshino, Walter & Katsura 2003; Neumann, Breuer & Spohn 2014), and this implies very large Rayleigh number (up to 10^{22}), i.e. a convective turbulent regime (Niemela et al. 2000). Core viscosity does not has a monotone profile since it reflects the behaviour of the core temperature that initially increases and, after reaching a maximum around 1400 K, decreases (see Fig. 7b). The maximum core viscosity value reached is 10^{14} Pa s, which corresponds to the typical value of the inner solid Earth's core viscosity (Koot & Dumberry 2011). Core viscosity follows the same exponential law valid for the mantle (equation 9), where the constant C is set to 90 to make it possible that viscosity reaches low value (10^{-2}–10^{-3} Pa s) when core was melted.

The melting constant C significantly influences the minimum value of the core viscosity. In order to obtain values compatible with the typical ones used in the literature for melt 'metals', C has to range from 85 to 95. The minimum value of the core viscosity increases if C overcomes 95 and decreases if C is less than 85. So small values of C characterize low-intensity magnetic field and a short dynamo duration; instead, high values of C lead to very intense magnetic field and long dynamo duration.

In Fig. 8, we can observe the time evolution of the core melt fraction, which exhibits an opposite trend compared to the core viscosity.

In a turbulent regime we can write, following (Jones 2007), a relationship between Nusselt and Rayleigh numbers:

$$\mathrm{Nu} \approx 0.066\mathrm{Ra}^{1/3}, \tag{45}$$

and the boundary layer at the top of the core is given by

$$\delta_c \approx \frac{0.5R_c}{\mathrm{Nu}}, \tag{46}$$

so the heat core flux is provided by

$$F_c = \frac{K\,(T_c - T_m)}{\delta_c}. \tag{47}$$

When viscosity becomes very low, the heat core flux jumps at very high value 10^4 mW m^{-2} and rapidly decreases when viscosity reaches its asymptotic value of 10^{14} Pa s (Fig. 7b). The mantle and crust heat fluxes are the same as the isoviscous core case previously examined (Figs 2c and 7c). In the turbulent regime of the core convection, the Nusselt number of the core reaches very high value (10^4; Niemela et al. 2000), as we can see in Fig. 7(d). Magnetic Reynolds number exceeds 10^3 (Fig. 7e) for a very narrow timespan and the duration of the dynamo is <200 Myr, which is the time interval during which the magnetic Reynolds number is larger than the critical value. The same behaviour is shown by the intensity of the magnetic fields (core and surface), as we can observe in Fig. 7(e). The maximum intensity of the core magnetic field is slightly lower than 10^4 μT for very short almost 'impulsive' time interval. This time interval, after about 30 Myr, could be interpreted as the time of the first magnetization of the rocks of the crust of Vesta.

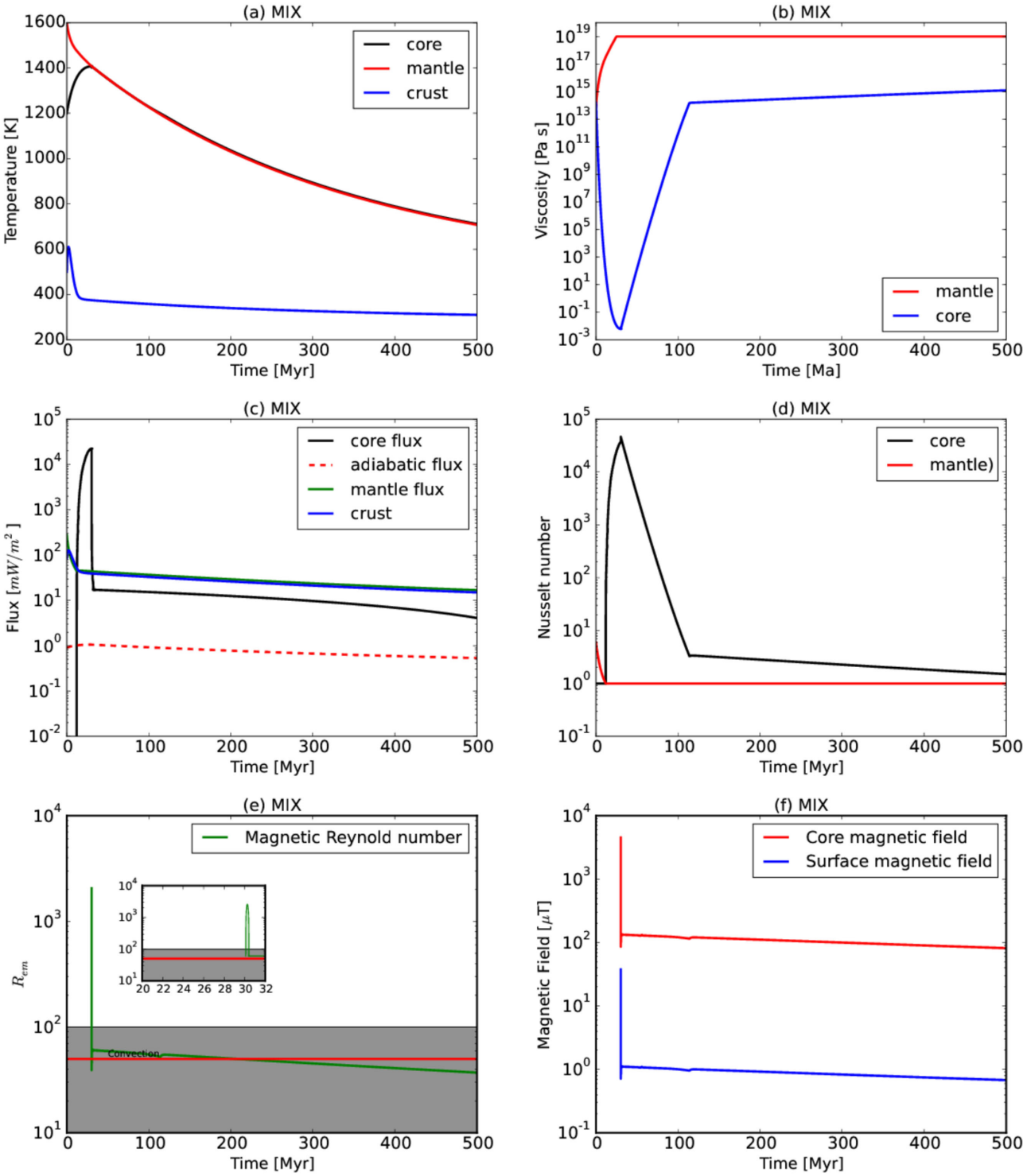

Figure 7. Time evolution of (a) temperature of different layers, (b) viscosity of mantle, (c) flux coming out of different layers and adiabatic core flux, (d) Nusselt number of mantle, (e) magnetic Reynolds number, (f) magnetic field intensity, in the case of Mod. A and mixing-length theory scaling law for core convective velocity and not isoviscous core. Grey box ranges from 10 to 100 which are the typical minimum and maximum values of the critical number we found in the literature. In our work, we set the critical value at 50 (red line).

6 DISCUSSION

In this work, we investigated, in a thermal convective regime, the possibility that Vesta had an active core dynamo in the first phases of its evolution, in order to explain the remaining magnetization found in the eucrite Allan Hills A81001 by Fu et al. (2012) and due to a magnetic field of at least 2 μT. We have used Vesta interior models present in the literature and based on the results obtained interpreting data coming from *Dawn* mission. These results show that Vesta had an earlier advective liquid metallic core in order to provide a dynamo effect, since the primitive magnetic field due to

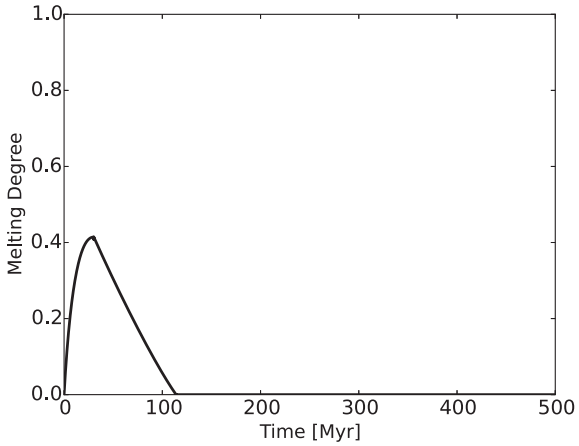

Figure 8. Core melt fraction time evolution.

the solar nebula decays in a short time (10^3–10^4 yr) with respect to the age of the Solar system and so it is not adequate to explain any remaining magnetization. If Vesta did not reach the Curie temperature of the crust materials (the Curie temperature of kamacite is around 760 °C), an ancient magnetization is preserved. In the inner structure (core and mantle), due to the high temperatures predicted by the numerical thermal models (Formisano et al. 2013; Neumann et al. 2014), any remaining magnetization is lost.

On the basis of petrological and geochemical considerations (Toplis et al. 2013) and with the constraints on the core size and density given by gravity measurements (Ermakov et al. 2014), we test four chondritic configurations, studying the magnetic Reynolds number and the consequent magnetic field. Our reference model is Mod. A, which is characterized by a chondritic composition made of 3/4 of H chondrite and 1/4 of CM chondrite (Toplis et al. 2013), which is a plausible configuration for a fully differentiated Vesta. In the reference Mod. A, the core velocity is given by the mixing-length theory and, after 30 Myr, the heat coming from the core is greater than the adiabatic flux: this is the requirement to have a convective core. The magnetic Reynolds number is greater than the critical value until about 200 Myr, which corresponds to a dynamo duration of about 150 Myr. Our results suggest also that a MAC scaling law is not adequate to treat the convective core velocity, since the magnetostrophic balance is not assured. The core magnetic field, in Mod. A, is around 10^2 μT, with a corresponding surface field of 1–2 μT. A change in the structure, in particular an increase of the core size (Mod. C and Mod. D), does not significantly affect the magnetic fields but affects the dynamo duration, which increases up to about 500 Myr. In contrast, a smaller core size (Mod. B) does not imply a core dynamo. The Rossby number, being lower than 0.12, indicates that the field is dipolar.

In the case of temperature-dependent core viscosity, the core magnetic field reaches value, when the dynamo was active, around 1000 μT, compatible with the estimation of Fu et al. (2012), which predicts fields with intensity up to 2600 μT. Also the surface fields reach values (up to 100 μT) compatible with the values provided by Fu et al. (2012). In summary, our simulations suggest that

(i) Vesta had an active core dynamo, whose duration lies in the range 150–500 Myr, depending on the internal structures;

(ii) the core viscosity is a crucial parameter in the generation of the magnetic field;

(iii) in the case of temperature-dependent viscosity, we obtain magnetic fields compatible with the measurement of the remaining magnetization in the eucrite meteorite sample (Fu et al. 2012);

(iv) in the case of low core viscosity, the generation of the magnetic field is 'impulsive';

(v) a MAC scaling law is not adequate for Vesta, for which a convective core velocity given by the mixing-length theory is more plausible.

It is also desirable that further laboratory investigations will be carried out on meteorites, with the aim to retrieve any eventual remnant magnetization.

ACKNOWLEDGEMENTS

This work is supported by an ASI grant. We are greatly indebted to Dr Roger R. Fu for his helpful comments and suggestions.

REFERENCES

Bryson J. F. J. et al., 2015, Nature, 517, 472
Christensen U. R., 2010, Space Sci. Rev., 152, 565
Christensen U. R., Aubert J., 2006, Geophys. J. Int., 166, 97
Christensen U., Olson P., Glatzmaier G. A., 1999, Geophys. J. Int., 138, 393
Elkins-Tanton L. T., Weiss B. P., Zuber M. T., 2011, Earth Planet. Sci. Lett., 305, 1
Ellsworth K., Schubert G., 1983, Icarus, 54, 490
Ermakov A. I., Zuber M. T., Smith D. E., Raymond C. A., Balmino G., Fu R. R., Ivanov B. A., 2014, Icarus, 240, 146
Formisano M., Federico C., Turrini D., Coradini A., Capaccioni F., De Sanctis M. C., Pauselli C., 2013, Meteorit. Planet. Sci., 48, 2316
Fraeman A. A., Korenaga J., 2010, Icarus, 210, 43
Freeman J., 2006, Planet. Space Sci., 54, 2
Fu R. R. et al., 2012, Science, 338, 238
Fu R. R., Hager B. H., Ermakov A. I., Zuber M. T., 2014a, Icarus, 240, 133
Fu R. R. et al., 2014b, Science, 346, 1089
Ghosh A., McSween H. Y., 1998, Icarus, 134, 187
Grindrod P. M., Fortes A. D., Nimmo F., Feltham D. L., Brodholt J. P., Vocadlo L., 2007, in European Planetary Science Congress 2007, p. 664, Available at http://meetings.copernicus.org/epsc2007
Jones C., 2007, in Schubert G., ed., Treatise on Geophysics. Elsevier, Amsterdam, p. 131
Koot L., Dumberry M., 2011, Earth Planet. Sci. Lett., 308, 343
Korenaga J., 2009, Geophys. J. Int., 179, 154
Korenaga J., Jordan T. H., 2002, Geophys. Res. Lett., 29, 1923
Levy E. H., Sonett C. P., 1978, in Gehrels T., ed., IAU Colloq. 52: Protostars and Planets. Univ. Arizona Press, Tucson, p. 516
McNamara A. K., van Keken P. E., 2000, Geochem. Geophys. Geosyst., 1, 1027
Monteux J., Jellinek A. M., Johnson C. L., 2011, Earth Planet. Sci. Lett., 310, 349
Moresi L., Solomatov V. S., 1995, Phys. Fluids, 7, 2154
Neumann W., Breuer D., Spohn T., 2014, Earth Planet. Sci. Lett., 395, 267
Niemela J. J., Skrbek L., Sreenivasan K. R., Donnelly R. J., 2000, Nature, 404, 837
Nimmo F., 2007, in Schubert G., ed., Treatise on Geophysics, Elsevier, Amsterdam, p. 31
Nimmo F., 2009, Geophys. Res. Lett., 36, 10201
Olson P., Christensen U. R., 2006, Earth Planet. Sci. Lett., 250, 561
Pieters C. M. et al., 2012, Nature, 491, 79
Reese C., Solomatov V., 2006, Icarus, 184, 102
Russell C. T. et al., 2012, Science, 336, 684
Schubert G., 1979, Annu. Rev. Earth Planet. Sci., 7, 289
Solomatov V. S., 1995, Phys. Fluids, 7, 266
Solomatov V. S., Moresi L.-N., 2000, J. Geophys. Res., 105, 21795
Starchenko S. V., Jones C. A., 2002, Icarus, 157, 426

Sterenborg G., Crowley J. W., 2013, Phys. Earth Planet. Inter., 214, 53
Stevenson D. J., 2003, Earth Planet. Sci. Lett., 208, 1
Stevenson D. J., 2010, Space Sci. Rev., 152, 651
Stevenson D. J., Spohn T., Schubert G., 1983, Icarus, 54, 466
Toplis M. J. et al., 2013, Meteorit. Planet. Sci., 48, 2300
Turcotte D., Schubert G., 2002, Geodynamics. Cambridge Univ. Press, Cambridge
Vernazza P., Brunetto R., Strazzulla G., Fulchignoni M., Rochette P., Meyer-Vernet N., Zouganelis I., 2006, A&A, 451, L43
Weiss B. P., Berdahl J. S., Elkins-Tanton L., Stanley S., Lima E. A., Carporzen L., 2008a, Science, 322, 713
Weiss B. P., Lima E. A., Zucolotto M. E., 2008b, in Lunar and Planetary Inst. Technical Report, Vol. 39, Lunar and Planetary Science Conference, p. 2143
Weiss B. P., Gattacceca J., Stanley S., Rochette P., Christensen U. R., 2010, Space Sci. Rev., 152, 341
Yoshino T., Walter M. J., Katsura T., 2003, Nature, 422, 154
Yoshino T., Walter M. J., Katsura T., 2004, Earth Planet. Sci. Lett., 222, 625

This paper has been typeset from a TEX/LATEX file prepared by the author.